Sequential Phase Linking: Progressive Integration of SAR Images for Operational Phase Estimation

Dana El Hajjar[1,2], Yajing Yan[1], Guillaume Ginolhac[1], Mohammed Nabil El Korso[2]

[1] Computer Science Laboratory, Systems, Information and Knowledge Processing (LISTIC)
[2] Laboratory of signals and systems (L2S)

23-29 June, 2024

Content

1. SAR interferometry
2. Phase Linking (PL)
3. Sequential Phase Linking based on Maximum Likelihood Estimation (S-MLE-PL)
4. Experiments
5. Area of study
6. Conclusion

Content

1. SAR interferometry
2. Phase Linking (PL)
3. Sequential Phase Linking based on Maximum Likelihood Estimation (S-MLE-PL)
4. Experiments
5. Area of study
6. Conclusion

SAR Image

Single Look Complex (SLC) is characterized by a complex signal $z = a \cdot e^{j\theta}$

SAR Image

Single Look Complex (SLC) is characterized by a complex signal $z = a \cdot e^{j\theta}$

- **Amplitude (a)**: intensity of the backscattering

SAR Image

Single Look Complex (SLC) is characterized by a complex signal $z = a \cdot e^{j\theta}$

- **Amplitude (a)**: intensity of the backscattering
- **Phase (θ)**: geometric information, random information
  $\theta = \theta_{\text{random}} + \theta_{\text{geometric}}$

SAR Image

Single Look Complex (SLC) is characterized by a complex signal $z = a \cdot e^{j\theta}$

- **Amplitude (a)**: intensity of the backscattering
- **Phase (θ)**: geometric information, random information
  $\theta = \theta_{\text{random}} + \theta_{\text{geometric}}$

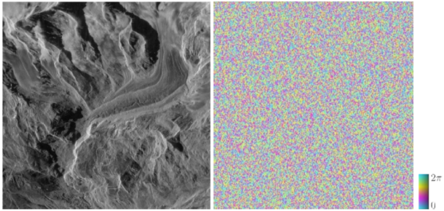

Sentinel-1 SAR image - glacier

Interferogram

2 SLC images of the same scene at different times → interferogram :

$$\gamma e^{j\theta}(i,j) = \frac{\sum_{i,j\in\Omega} z_1(i,j) z_2^*(i,j)}{\sqrt{\sum_{i,j\in\Omega} z_1(i,j) z_1^*(i,j) \sum_{i,j\in\Omega} z_2(i,j) z_2^*(i,j)}}$$

Interferogram

2 SLC images of the same scene at different times → interferogram :

$$\gamma e^{j\theta}(i,j) = \frac{\sum_{i,j\in\Omega} z_1(i,j) z_2^*(i,j)}{\sqrt{\sum_{i,j\in\Omega} z_1(i,j) z_1^*(i,j) \sum_{i,j\in\Omega} z_2(i,j) z_2^*(i,j)}}$$

where:

- γ is **coherence** ($\in [0,1]$), representing the similarity between the two images

Interferogram

2 SLC images of the same scene at different times → interferogram :

$$\gamma e^{j\theta}(i,j) = \frac{\sum_{i,j\in\Omega} z_1(i,j) z_2^*(i,j)}{\sqrt{\sum_{i,j\in\Omega} z_1(i,j) z_1^*(i,j) \sum_{i,j\in\Omega} z_2(i,j) z_2^*(i,j)}}$$

where:

- γ is **coherence** ($\in [0,1]$), representing the similarity between the two images
- θ represents the **phase difference** ($\theta = \theta_1 - \theta_2$, $\theta \in [-\pi, \pi]$)

Interferogram

2 SLC images of the same scene at different times $\rightarrow$ interferogram :

$$\gamma e^{j\theta}(i,j) = \frac{\sum_{i,j\in\Omega} z_1(i,j) z_2^*(i,j)}{\sqrt{\sum_{i,j\in\Omega} z_1(i,j) z_1^*(i,j) \sum_{i,j\in\Omega} z_2(i,j) z_2^*(i,j)}}$$

where:

- γ is **coherence** ($\in [0,1]$), representing the similarity between the two images
- θ represents the **phase difference** ($\theta = \theta_1 - \theta_2$, $\theta \in [-\pi, \pi]$)

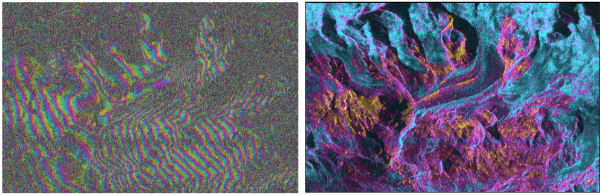

(a) phase (b) coherence

Interferometric phase

$$\theta = \frac{4\pi}{\lambda}\frac{B_\perp}{R_m \sin(\alpha)} h + \frac{4\pi}{\lambda} d_{LOS}$$

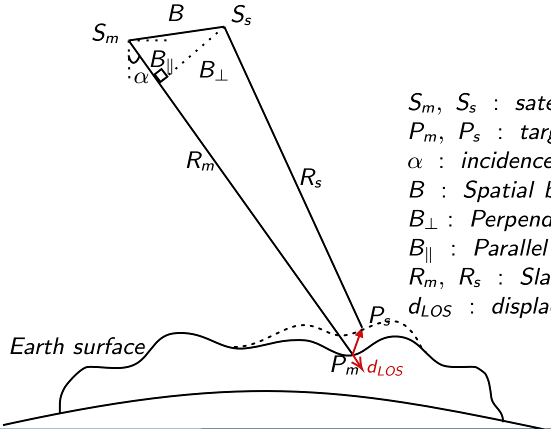

S_m, S_s : *satellites position*
P_m, P_s : *target positions*
α : *incidence angle*
B : *Spatial baseline*
$B_\perp$: *Perpendicular baseline*
$B_{\|}$: *Parallel baseline*
R_m, R_s : *Slant ranges*
d_{LOS} : *displacement in line of sight*

Multi-temporal InSAR

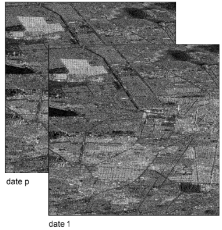

Interferogram of 2 SLC images

- Unsatisfactory results
- Measurement accuracy (centimetric)

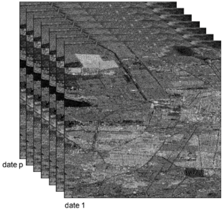

Multi-temporal interferograms

- Continuous monitoring of Earth deformations
- Improvement in measurement accuracy (millimetric)
- Building interferometric networks from a time series of SAR images

Content

Data model

Consider a multivariate random vector $\widetilde{\mathbf{x}} = [\widetilde{x}_1, \ldots, \widetilde{x}_p]^T$ for all $(l, k) \in [0, p-1]^2$.

$$\mathbb{E}[\widetilde{x}_l(\widetilde{x}_k)^*] = \gamma_{k,l}\sigma_k\sigma_l \exp(j(\theta_l - \theta_k))$$

$$\boxed{\mathbb{E}[\widetilde{\mathbf{x}}\widetilde{\mathbf{x}}^H] \triangleq \widetilde{\boldsymbol{\Sigma}} = \widetilde{\boldsymbol{\Psi}} \odot \widetilde{\mathbf{w}}_\theta \widetilde{\mathbf{w}}_\theta^H} \tag{1}$$

with:

- $\gamma_{k,l}$: correlation coefficient between $\widetilde{x}_k$ and $\widetilde{x}_l$
- σ_l: standard deviation of $\widetilde{x}_l$
- $\widetilde{\boldsymbol{\Psi}}$: coherence matrix
- $\widetilde{\mathbf{w}}_\theta$: vector of phase exponential

Gaussian Distribution

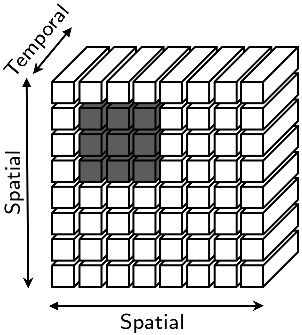

Representation of SAR time series using a sliding window of n pixels $\widetilde{x}^i$ [6]

[6] P. Vu, A. Breloy, F. Brigui, Y. Yan, and G. Ginolhac, "A new phase linking algorithm for multi-temporal INSAR based on the maximum likelihood estimator" IGARSS International Geoscience and Remote Sensing Symposium, IEEE, 2022

Gaussian Distribution

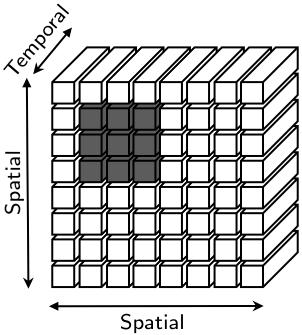

Representation of SAR time series using a sliding window of n pixels $\widetilde{x}^i$ [6]

Consider a set $\{\widetilde{\mathbf{x}}^i\}_{i=1}^n$ with $\widetilde{\mathbf{x}}^i \in \mathbb{C}^p \ \forall i \in [1, n]$, independently and identically distributed $\longrightarrow \widetilde{\mathbf{x}} \sim \mathcal{CN}(0, \widetilde{\boldsymbol{\Sigma}})$

[6] P. Vu, A. Breloy, F. Brigui, Y. Yan, and G. Ginolhac, "A new phase linking algorithm for multi-temporal INSAR based on the maximum likelihood estimator" IGARSS International Geoscience and Remote Sensing Symposium, IEEE, 2022

Gaussian Distribution

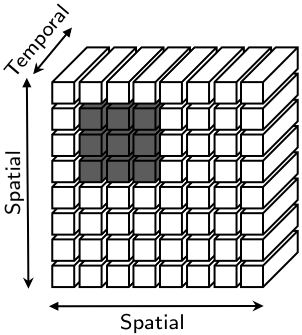

Representation of SAR time series using a sliding window of n pixels $\widetilde{x}^i$ [6]

Consider a set $\{\widetilde{\mathbf{x}}^i\}_{i=1}^n$ with $\widetilde{\mathbf{x}}^i \in \mathbb{C}^p \ \forall i \in [1, n]$, independently and identically distributed $\longrightarrow \widetilde{\mathbf{x}} \sim \mathcal{CN}(0, \widetilde{\boldsymbol{\Sigma}})$

The log-likelihood is

$$\mathcal{L}(\widetilde{\mathbf{x}}; \widetilde{\boldsymbol{\Sigma}}) = -\log\left(\prod_{i=1}^n f(\widetilde{\mathbf{x}}^i, \widetilde{\boldsymbol{\Sigma}})\right)$$
$$\propto n\log(|\widetilde{\boldsymbol{\Sigma}}|) + n\,\mathrm{Tr}(\widetilde{\boldsymbol{\Sigma}}^{-1}\mathbf{S})$$

where $\mathbf{S} = \frac{1}{n}\sum_{i=1}^n \widetilde{\mathbf{x}}^i \widetilde{\mathbf{x}}^{iH}$

[6] P. Vu, A. Breloy, F. Brigui, Y. Yan, and G. Ginolhac, "A new phase linking algorithm for multi-temporal INSAR based on the maximum likelihood estimator" IGARSS International Geoscience and Remote Sensing Symposium, IEEE, 2022

Gaussian Distribution

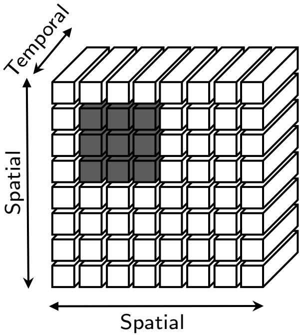

Representation of SAR time series using a sliding window of n pixels $\widetilde{x}^i$ [6]

Consider a set $\{\widetilde{\mathbf{x}}^i\}_{i=1}^n$ with $\widetilde{\mathbf{x}}^i \in \mathbb{C}^p \ \forall i \in [1, n]$, independently and identically distributed $\longrightarrow \widetilde{\mathbf{x}} \sim \mathcal{CN}(0, \widetilde{\boldsymbol{\Sigma}})$

The log-likelihood is

$$\mathcal{L}(\widetilde{\mathbf{x}}; \widetilde{\boldsymbol{\Sigma}}) = -\log\left(\prod_{i=1}^{n} f(\widetilde{\mathbf{x}}^i, \widetilde{\boldsymbol{\Sigma}})\right)$$
$$\propto n\log(|\widetilde{\boldsymbol{\Sigma}}|) + n\,\mathrm{Tr}(\widetilde{\boldsymbol{\Sigma}}^{-1}\mathbf{S})$$

where $\mathbf{S} = \frac{1}{n}\sum_{i=1}^{n} \widetilde{\mathbf{x}}^i \widetilde{\mathbf{x}}^{iH}$

$\boxed{n > p}$

[6] P. Vu, A. Breloy, F. Brigui, Y. Yan, and G. Ginolhac, "A new phase linking algorithm for multi-temporal INSAR based on the maximum likelihood estimator" IGARSS International Geoscience and Remote Sensing Symposium, IEEE, 2022

Classic PL

Principle:
Estimate $p-1$ phase differences from p SAR images.

[2] Guarnieri, Andrea Monti, and Stefano Tebaldini. "On the exploitation of target statistics for SAR interferometry applications." IEEE Transactions on Geoscience and Remote Sensing 46.11 (2008): 3436-3443.

[6] P. Vu, A. Breloy, F. Brigui, Y. Yan, and G. Ginolhac, "A new phase linking algorithm for multi-temporal INSAR based on the maximum likelihood estimator" IGARSS International Geoscience and Remote Sensing Symposium, IEEE, 2022

Classic PL

Principle:
Estimate $p-1$ phase differences from p SAR images.

Assuming that $\widetilde{\boldsymbol{\Psi}}$ is known, the method is equivalent to optimizing the following problem [2]:

$$\begin{aligned} \underset{\widetilde{\mathbf{w}}_\theta}{\text{minimize}} \quad & \widetilde{\mathbf{w}}_\theta^H (\widetilde{\boldsymbol{\Psi}}^{-1} \circ \mathbf{S}) \widetilde{\mathbf{w}}_\theta \\ \text{subject to} \quad & \theta_1 = 0 \end{aligned} \tag{2}$$

[2] Guarnieri, Andrea Monti, and Stefano Tebaldini. "On the exploitation of target statistics for SAR interferometry applications." IEEE Transactions on Geoscience and Remote Sensing 46.11 (2008): 3436-3443.

[6] P. Vu, A. Breloy, F. Brigui, Y. Yan, and G. Ginolhac, "A new phase linking algorithm for multi-temporal INSAR based on the maximum likelihood estimator" IGARSS International Geoscience and Remote Sensing Symposium, IEEE, 2022

Classic PL

Principle:
Estimate $p-1$ phase differences from p SAR images.

Assuming that $\widetilde{\boldsymbol{\Psi}}$ is known, the method is equivalent to optimizing the following problem [2]:

$$\begin{aligned} \underset{\widetilde{\mathbf{w}}_\theta}{\text{minimize}} \quad & \widetilde{\mathbf{w}}_\theta^H(\widetilde{\boldsymbol{\Psi}}^{-1} \circ \mathbf{S})\widetilde{\mathbf{w}}_\theta \\ \text{subject to} \quad & \theta_1 = 0 \end{aligned} \tag{2}$$

PROBLEM !!!
In reality, $\widetilde{\boldsymbol{\Psi}}$ is unknown

- [2] proposed to use a plug-in: $\widetilde{\boldsymbol{\Psi}}_{mod} = |\mathbf{S}| \longrightarrow$ **not optimal**
- [6] proposed to estimate $\widetilde{\boldsymbol{\Psi}}$ jointly with $\widetilde{\mathbf{w}}_\theta$

[2] Guarnieri, Andrea Monti, and Stefano Tebaldini. "On the exploitation of target statistics for SAR interferometry applications." IEEE Transactions on Geoscience and Remote Sensing 46.11 (2008): 3436-3443.

[6] P. Vu, A. Breloy, F. Brigui, Y. Yan, and G. Ginolhac, "A new phase linking algorithm for multi-temporal INSAR based on the maximum likelihood estimator" IGARSS International Geoscience and Remote Sensing Symposium, IEEE, 2022

Phase Linking based on Maximum Likelihood Estimation (MLE-PL)

→ The optimization problem [6]:

$$
\begin{array}{ll}
\underset{\widetilde{\boldsymbol{\Psi}}, \widetilde{\mathbf{w}}_\theta}{\text{minimize}} & \mathcal{L}_{\mathcal{G}}(\widetilde{\mathbf{x}}^i; \widetilde{\boldsymbol{\Sigma}}(\widetilde{\boldsymbol{\Psi}}, \widetilde{\mathbf{w}}_\theta)) \\
 & = n \log(|\widetilde{\boldsymbol{\Sigma}}|) + \sum_{i=1}^{n} \widetilde{\mathbf{x}}^{iH} \widetilde{\boldsymbol{\Sigma}}^{-1} \widetilde{\mathbf{x}}^i \\
\text{subject to} & \theta_1 = 0 \\
 & \widetilde{\mathbf{w}}_\theta \in \mathbb{T}_p \\
 & \widetilde{\boldsymbol{\Psi}} \text{ real symmetric}
\end{array}
$$

with $\mathbb{T}_p = \{\widetilde{\mathbf{w}} \in \mathbb{C}^p || [\widetilde{w}]_i| = 1, \forall i \in [1, p]\}$

[6] P. Vu, A. Breloy, F. Brigui, Y. Yan, and G. Ginolhac. "A new phase linking algorithm for multi-temporal INSAR based on the maximum likelihood estimator." IGARSS International Geoscience and Remote Sensing Symposium. IEEE, 2022.

Phase Linking based on Maximum Likelihood Estimation (MLE-PL)

→ The optimization problem [6]:

$$\begin{aligned} \underset{\widetilde{\boldsymbol{\Psi}},\widetilde{\mathbf{w}}_\theta}{\text{minimize}} \quad & \mathcal{L}_{\mathcal{G}}(\widetilde{\mathbf{x}}^i; \widetilde{\boldsymbol{\Sigma}}(\widetilde{\boldsymbol{\Psi}}, \widetilde{\mathbf{w}}_\theta)) \\ & = n \log(|\widetilde{\boldsymbol{\Sigma}}|) + \sum_{i=1}^{n} \widetilde{\mathbf{x}}^{iH} \widetilde{\boldsymbol{\Sigma}}^{-1} \widetilde{\mathbf{x}}^i \\ \text{subject to} \quad & \theta_1 = 0 \\ & \widetilde{\mathbf{w}}_\theta \in \mathbb{T}_p \\ & \widetilde{\boldsymbol{\Psi}} \text{ real symmetric} \end{aligned}$$

with $\mathbb{T}_p = \{\widetilde{\mathbf{w}} \in \mathbb{C}^p || [\widetilde{w}]_i| = 1, \forall i \in [1, p]\}$

2 unknowns to estimate ⟶ **Block Coordinate Descent Algorithm (BCD)**

[6] P. Vu, A. Breloy, F. Brigui, Y. Yan, and G. Ginolhac. "A new phase linking algorithm for multi-temporal INSAR based on the maximum likelihood estimator." IGARSS International Geoscience and Remote Sensing Symposium. IEEE, 2022.

Phase Linking based on Maximum Likelihood Estimation (MLE-PL)

→ The optimization problem [6]:

$$\begin{array}{ll} \underset{\widetilde{\boldsymbol{\Psi}}, \widetilde{\mathbf{w}}_\theta}{\text{minimize}} & \mathcal{L}_{\mathcal{G}}(\widetilde{\mathbf{x}}^i; \widetilde{\boldsymbol{\Sigma}}(\widetilde{\boldsymbol{\Psi}}, \widetilde{\mathbf{w}}_\theta)) \\ & = n \log(|\widetilde{\boldsymbol{\Sigma}}|) + \sum_{i=1}^{n} \widetilde{\mathbf{x}}^{iH} \widetilde{\boldsymbol{\Sigma}}^{-1} \widetilde{\mathbf{x}}^i \\ \text{subject to} & \theta_1 = 0 \\ & \widetilde{\mathbf{w}}_\theta \in \mathbb{T}_p \\ & \widetilde{\boldsymbol{\Psi}} \text{ real symmetric} \end{array}$$

with $\mathbb{T}_p = \{\widetilde{\mathbf{w}} \in \mathbb{C}^p \,||[\widetilde{w}]_i| = 1, \forall i \in [1, p]\}$

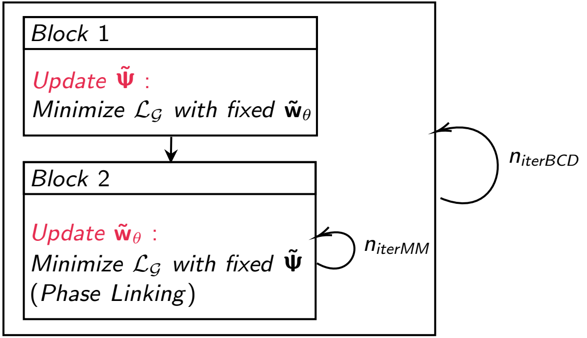

2 unknowns to estimate ⟶ **Block Coordinate Descent Algorithm (BCD)**

[6] P. Vu, A. Breloy, F. Brigui, Y. Yan, and G. Ginolhac. "A new phase linking algorithm for multi-temporal INSAR based on the maximum likelihood estimator." IGARSS International Geoscience and Remote Sensing Symposium. IEEE, 2022.

Content

1. SAR interferometry
2. Phase Linking (PL)
3. Sequential Phase Linking based on Maximum Likelihood Estimation (S-MLE-PL)
4. Experiments
5. Area of study
6. Conclusion

A new image arrives

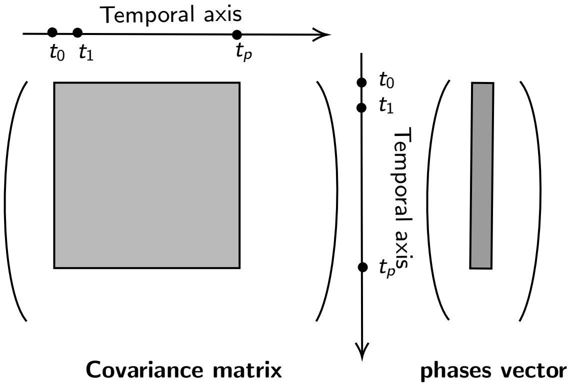

$$\forall i = 1, \dots, n$$

$$\tilde{\mathbf{x}}^i = \begin{pmatrix} x_1^i \\ x_2^i \\ \vdots \\ x_p^i \end{pmatrix}_{(p,1)}$$

A new image arrives

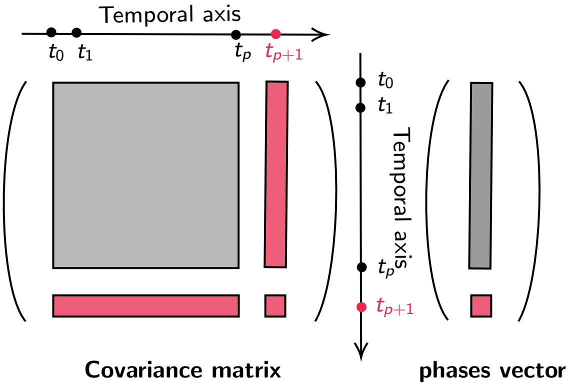

$\forall i = 1, \dots, n$

$$\tilde{\mathbf{x}}^i = \begin{pmatrix} x_1^i \\ x_2^i \\ \vdots \\ x_p^i \end{pmatrix}_{(p,1)} \rightarrow \quad \tilde{\mathbf{x}}^i = \begin{pmatrix} x_1^i \\ x_2^i \\ \vdots \\ x_p^i \\ \mathbf{x}_{p+1}^i \end{pmatrix}_{(p+1,1)}$$

At each new SAR acquisition,

- Re-Estimation of the increasing covariance matrix
- Re-Estimation of the phases

$\longrightarrow$ **Huge computation time**

A new image arrives

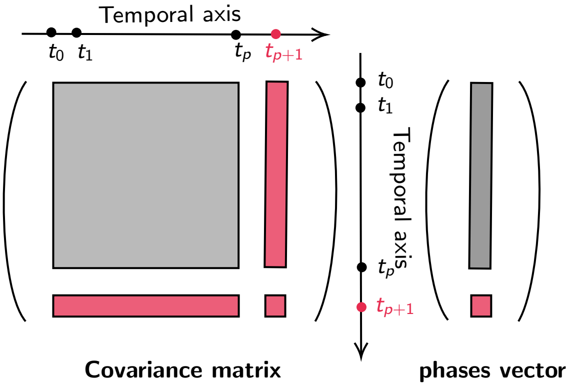

$\forall i = 1, \ldots, n$

$$\tilde{\mathbf{x}}^i = \begin{pmatrix} x_1^i \\ x_2^i \\ \vdots \\ x_p^i \end{pmatrix}_{(p,1)} \rightarrow \quad \tilde{\mathbf{x}}^i = \begin{pmatrix} x_1^i \\ x_2^i \\ \vdots \\ x_p^i \\ \mathbf{x}_{p+1}^i \end{pmatrix}_{(p+1,1)}$$

At each new SAR acquisition,

- Re-Estimation of the increasing covariance matrix
- Re-Estimation of the phases

$\longrightarrow$ **Huge computation time**

Problem : Development of a new, robust and sequential multi-temporal SAR interferometry approach for estimating SAR phase time series using statistical tools.

Data model

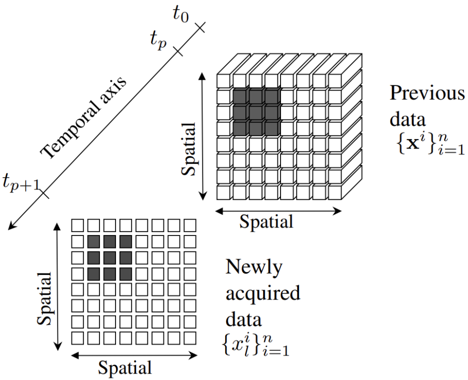

Representation of SAR time series with a sliding window containing n pixels $\tilde{x}^i$ [3]

We consider a set $\{\tilde{\mathbf{x}}^i\}_{i=1}^n$ where

$$\tilde{\mathbf{x}}^i = [\underbrace{x_1^i, \ldots, x_p^i}_{\mathbf{x}^i}, x_l^i]^T \in \mathbb{C}^{l=p+1} \tag{3}$$

Data model

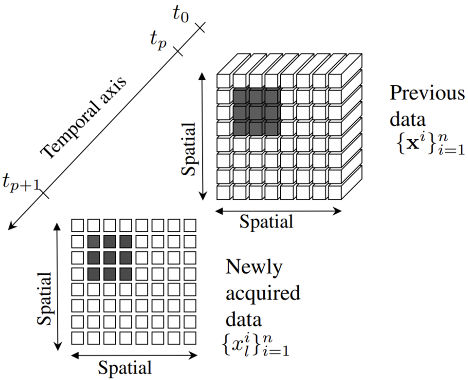

Representation of SAR time series with a sliding window containing n pixels $\widetilde{x}^i$ [3]

We consider a set $\{\widetilde{\mathbf{x}}^i\}_{i=1}^n$ where

$$\widetilde{\mathbf{x}}^i = [\underbrace{x_1^i, \ldots, x_p^i}_{\mathbf{x}^i}, x_l^i]^T \in \mathbb{C}^{l=p+1} \tag{3}$$

Each pixel of the local patch is assumed to be distributed as a zero mean CCG, i.e., $\widetilde{\mathbf{x}} \sim \mathcal{CN}(0, \widetilde{\boldsymbol{\Sigma}})$.

Data model

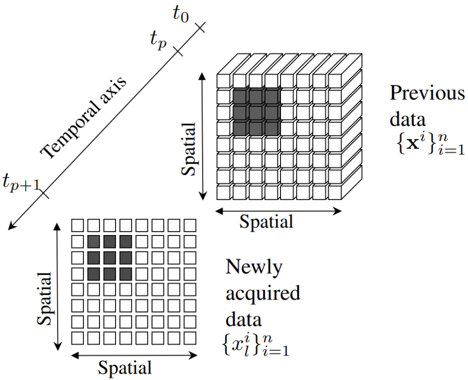

Representation of SAR time series with a sliding window containing n pixels $\widetilde{x}^i$ [3]

We consider a set $\{\widetilde{\mathbf{x}}^i\}_{i=1}^n$ where

$$\widetilde{\mathbf{x}}^i = [\underbrace{x_1^i, \ldots, x_p^i}_{\mathbf{x}^i}, x_l^i]^T \in \mathbb{C}^{l=p+1} \quad (3)$$

Each pixel of the local patch is assumed to be distributed as a zero mean CCG, i.e., $\widetilde{\mathbf{x}} \sim \mathcal{CN}(0, \widetilde{\boldsymbol{\Sigma}})$.

The hermitian structured covariance matrix, given in (1), can be rewritten as

$$\widetilde{\boldsymbol{\Sigma}} = \begin{pmatrix} \Sigma & w_{\theta_l}^* \mathrm{diag}(\mathbf{w}_\theta)\gamma^T \\ \gamma \mathrm{diag}(\mathbf{w}_\theta)^H w_{\theta_l} & \gamma_l \end{pmatrix} \quad (4)$$

Maximum Likelihood Estimation (MLE) problem

$$\begin{array}{ll} \underset{\tilde{\boldsymbol{\Psi}}, \tilde{\mathbf{w}}_\theta}{\text{minimize}} & \mathcal{L}_{\mathcal{G}}(\tilde{\mathbf{x}}^i; \tilde{\boldsymbol{\Sigma}}(\tilde{\boldsymbol{\Psi}}, \tilde{\mathbf{w}}_\theta)) \\ \text{subject to} & \theta_1 = 0, \tilde{\mathbf{w}}_\theta \in \mathbb{T}_p, \tilde{\boldsymbol{\Psi}} \text{real symmetric} \end{array}$$

[1] T. W. Anderson, An introduction to multivariate statistic analysis, vol. 2, Wiley New York, 1958.

MLE problem

$$\begin{array}{ll} \underset{\tilde{\boldsymbol{\Psi}}, \tilde{\mathbf{w}}_\theta}{\text{minimize}} & \mathcal{L}_\mathcal{G}(\tilde{\mathbf{x}}^i; \tilde{\boldsymbol{\Sigma}}(\tilde{\boldsymbol{\Psi}}, \tilde{\mathbf{w}}_\theta)) \\ \text{subject to} & \theta_1 = 0, \tilde{\mathbf{w}}_\theta \in \mathbb{T}_p, \tilde{\boldsymbol{\Psi}} \text{real symmetric} \end{array}$$

$$\begin{array}{ll} \underset{\gamma, \gamma_l, w_{\theta_l}}{\text{minimize}} & \mathcal{L}_\mathcal{G}(\tilde{\mathbf{x}}^i; \gamma, \gamma_l, w_{\theta_l}) \\ \text{subject to} & \gamma, \gamma_l \text{ real}, |w_{\theta_l}| = 1, \theta_1 = 0 \end{array}$$

[1] T. W. Anderson, An introduction to multivariate statistic analysis, vol. 2, Wiley New York, 1958.

MLE problem

$$\begin{aligned} \underset{\tilde{\boldsymbol{\Psi}}, \tilde{\mathbf{w}}_\theta}{\text{minimize}} \quad & \mathcal{L}_{\mathcal{G}}(\tilde{\mathbf{x}}^i; \tilde{\boldsymbol{\Sigma}}(\tilde{\boldsymbol{\Psi}}, \tilde{\mathbf{w}}_\theta)) \\ \text{subject to} \quad & \theta_1 = 0, \tilde{\mathbf{w}}_\theta \in \mathbb{T}_p, \tilde{\boldsymbol{\Psi}} \text{real symmetric} \end{aligned}$$

$$\begin{aligned} \underset{\gamma, \gamma_l, w_{\theta_l}}{\text{minimize}} \quad & \mathcal{L}_{\mathcal{G}}(\tilde{\mathbf{x}}^i; \gamma, \gamma_l, w_{\theta_l}) \\ \text{subject to} \quad & \gamma, \gamma_l \text{ real}, |w_{\theta_l}| = 1, \theta_1 = 0 \end{aligned}$$

$$\mathcal{L}_{\mathcal{G}}(\tilde{\mathbf{x}}^i; \gamma, \gamma_l, w_{\theta_l}) = -\sum_{i=1}^{n} \mathcal{L}_{\mathcal{G}}{}^i(x_l^i | \mathbf{x}^i; \gamma, \gamma_l, w_{\theta_l}) + \mathcal{L}_{\mathcal{G}}{}^i(\mathbf{x}^i)$$

[1] T. W. Anderson, An introduction to multivariate statistic analysis, vol. 2, Wiley New York, 1958.

MLE problem

$$\begin{aligned} \underset{\tilde{\boldsymbol{\Psi}}, \tilde{\mathbf{w}}_\theta}{\text{minimize}} \quad & \mathcal{L}_{\mathcal{G}}(\tilde{\mathbf{x}}^i; \tilde{\boldsymbol{\Sigma}}(\tilde{\boldsymbol{\Psi}}, \tilde{\mathbf{w}}_\theta)) \\ \text{subject to} \quad & \theta_1 = 0, \tilde{\mathbf{w}}_\theta \in \mathbb{T}_p, \tilde{\boldsymbol{\Psi}} \text{real symmetric} \end{aligned}$$

$$\begin{aligned} \underset{\gamma, \gamma_l, w_{\theta_l}}{\text{minimize}} \quad & \mathcal{L}_{\mathcal{G}}(\tilde{\mathbf{x}}^i; \gamma, \gamma_l, w_{\theta_l}) \\ \text{subject to} \quad & \gamma, \gamma_l \text{ real}, |w_{\theta_l}| = 1, \theta_1 = 0 \end{aligned}$$

$$\mathcal{L}_{\mathcal{G}}(\tilde{\mathbf{x}}^i; \gamma, \gamma_l, w_{\theta_l}) = -\sum_{i=1}^{n} \mathcal{L}_{\mathcal{G}}{}^i(x_l^i | \mathbf{x}^i; \gamma, \gamma_l, w_{\theta_l}) + \mathcal{L}_{\mathcal{G}}{}^i(\mathbf{x}^i)$$

According to [1], $x_l^i | \mathbf{x}^i \sim \mathcal{CN}(\mu_x^i, \sigma_x^2)$ where

$$\mu_x^i = w_{\theta_l} \gamma \operatorname{diag}(\hat{\mathbf{w}}_\theta)^H \hat{\boldsymbol{\Sigma}}^{-1} \mathbf{x}^i,$$
$$\sigma_x^2 = \gamma_l - \gamma \operatorname{diag}(\hat{\mathbf{w}}_\theta)^H \hat{\boldsymbol{\Sigma}}^{-1} \operatorname{diag}(\hat{\mathbf{w}}_\theta^H) \gamma^T \times$$

[1] T. W. Anderson, An introduction to multivariate statistic analysis, vol. 2, Wiley New York, 1958.

MLE problem

$$\begin{aligned} \underset{\tilde{\boldsymbol{\Psi}},\tilde{\mathbf{w}}_\theta}{\text{minimize}} \quad & \mathcal{L}_{\mathcal{G}}(\tilde{\mathbf{x}}^i; \tilde{\boldsymbol{\Sigma}}(\tilde{\boldsymbol{\Psi}}, \tilde{\mathbf{w}}_\theta)) \\ \text{subject to} \quad & \theta_1 = 0, \tilde{\mathbf{w}}_\theta \in \mathbb{T}_p, \tilde{\boldsymbol{\Psi}} \text{real symmetric} \end{aligned}$$

$$\begin{aligned} \underset{\boldsymbol{\gamma},\gamma_l,w_{\theta_l}}{\text{minimize}} \quad & \mathcal{L}_{\mathcal{G}}(\tilde{\mathbf{x}}^i; \boldsymbol{\gamma}, \gamma_l, w_{\theta_l}) \\ \text{subject to} \quad & \boldsymbol{\gamma}, \gamma_l \text{ real}, |w_{\theta_l}| = 1, \theta_1 = 0 \end{aligned}$$

Advantages for estimating w_θ :
- estimated phases
- new image data
- statistics of the conditional distribution of new image with respect to the past

$$\mathcal{L}_{\mathcal{G}}(\tilde{\mathbf{x}}^i; \boldsymbol{\gamma}, \gamma_l, w_{\theta_l}) = -\sum_{i=1}^{n} \mathcal{L}_{\mathcal{G}}{}^i(x_l^i | \mathbf{x}^i; \boldsymbol{\gamma}, \gamma_l, w_{\theta_l}) + \mathcal{L}_{\mathcal{G}}{}^i(\mathbf{x}^i)$$

According to [1], $x_l^i | \mathbf{x}^i \sim \mathcal{CN}(\mu_x^i, \sigma_x^2)$ where

$$\mu_x^i = w_{\theta_l} \boldsymbol{\gamma} \mathrm{diag}(\hat{\mathbf{w}}_\theta)^H \hat{\boldsymbol{\Sigma}}^{-1} \mathbf{x}^i,$$
$$\sigma_x^2 = \gamma_l - \boldsymbol{\gamma} \mathrm{diag}(\hat{\mathbf{w}}_\theta)^H \hat{\boldsymbol{\Sigma}}^{-1} \mathrm{diag}(\hat{\mathbf{w}}_\theta^H) \boldsymbol{\gamma}^T \times$$

[1] T. W. Anderson, An introduction to multivariate statistic analysis, vol. 2, Wiley New York, 1958.

MLE-PL vs S-MLE-PL

$$\underset{\gamma, \gamma_l, w_{\theta_l}}{\text{minimize}} \quad \mathcal{L}_{\mathcal{G}}(\tilde{\mathbf{x}}^i; \gamma, \gamma_l, w_{\theta_l})$$
$$\gamma, \gamma_l \text{ real}, |w_{\theta_l}| = 1, \theta_1 = 0$$

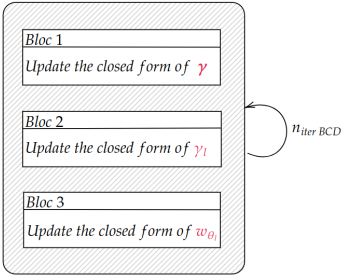

MLE-PL vs S-MLE-PL

$$\underset{\gamma, \gamma_l, w_{\theta_l}}{\text{minimize}} \quad \mathcal{L}_{\mathcal{G}}(\tilde{\mathbf{x}}^i; \gamma, \gamma_l, w_{\theta_l})$$
$$\gamma, \gamma_l \text{ real}, |w_{\theta_l}| = 1, \theta_1 = 0$$

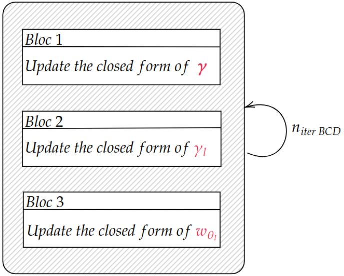

closed forms for each parameter, simple

MLE-PL vs S-MLE-PL

$$\underset{\tilde{\Psi},\tilde{\mathbf{w}}_\theta}{\text{minimize}} \quad \mathcal{L}_\mathcal{G}(\tilde{\mathbf{x}}^i; \tilde{\mathbf{\Sigma}}(\tilde{\Psi}, \tilde{\mathbf{w}}_\theta))$$
$$\theta_1 = 0, \tilde{\mathbf{w}}_\theta \in \mathbb{T}_p, \tilde{\Psi} \text{ real symmetric}$$

$$\underset{\gamma,\gamma_l,w_{\theta_l}}{\text{minimize}} \quad \mathcal{L}_\mathcal{G}(\tilde{\mathbf{x}}^i; \gamma, \gamma_l, w_{\theta_l})$$
$$\gamma, \gamma_l \text{ real}, |w_{\theta_l}| = 1, \theta_1 = 0$$

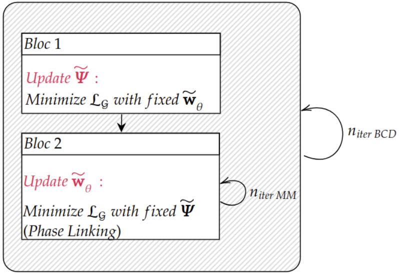

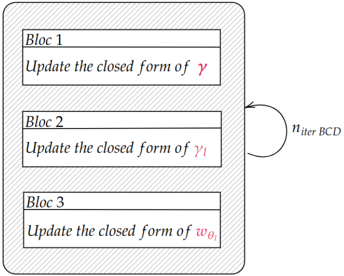

iterative algorithms, sophisticated

closed forms for each parameter, simple

Content

Simulation - Computation Time

S-MLE-PL	MLE-PL
$O(p^3)$	$O(n_{\text{iter}}\, p^3)$

Complexity comparison of S-MLE-PL and MLE-PL

Simulation - Computation Time

Simulation parameters

- $\widetilde{\mathbf{\Psi}}$: Toeplitz matrix with coherence coefficient $\rho = 0.7$
- $p + 1 = 20$ SAR phases: random values in $[-\pi, \pi]$
- Covariance matrix : $\widetilde{\mathbf{\Sigma}} = \text{diag}(\widetilde{\mathbf{w}}_\theta)\widetilde{\mathbf{\Psi}}\text{diag}(\widetilde{\mathbf{w}}_\theta)^H$
- n i.i.d samples simulated following the $\mathcal{CN}(0, \widetilde{\mathbf{\Sigma}})$

S-MLE-PL	MLE-PL
$O(p^3)$	$O(n_{\text{iter}}\, p^3)$

Complexity comparison of S-MLE-PL and MLE-PL

Simulation - Computation Time

Simulation parameters

- $\widetilde{\mathbf{\Psi}}$: Toeplitz matrix with coherence coefficient $\rho = 0.7$
- $p + 1 = 20$ SAR phases: random values in $[-\pi, \pi]$
- Covariance matrix : $\widetilde{\mathbf{\Sigma}} = \text{diag}(\widetilde{\mathbf{w}}_\theta)\widetilde{\mathbf{\Psi}}\text{diag}(\widetilde{\mathbf{w}}_\theta)^H$
- n i.i.d samples simulated following the $\mathcal{CN}(0, \widetilde{\mathbf{\Sigma}})$

S-MLE-PL	MLE-PL
$O(p^3)$	$O(n_{\text{iter}}\, p^3)$

Complexity comparison of S-MLE-PL and MLE-PL

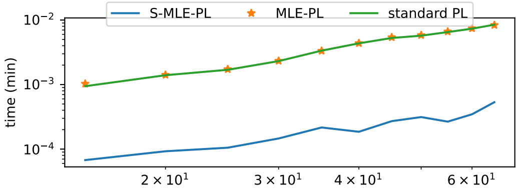

Computation time variation versus l, $n = 2 \times l$

Content

Real data - Mexico city

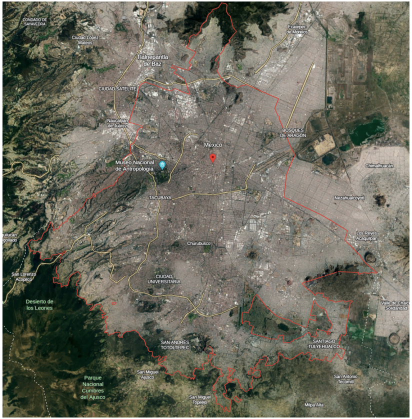

Mexico City

- population > 20M, highly dynamic
- rapid urbanization $\rightarrow$ increased water demand
- primary water from aquifers $\rightarrow$ subsidence and city deformation

Real data - Results

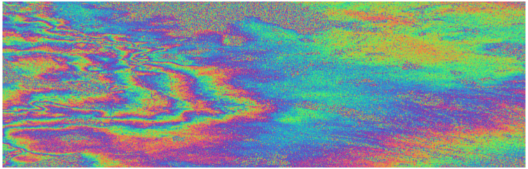

MLE-PL

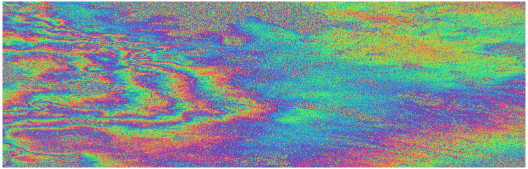

S-MLE-PL

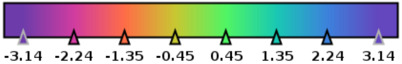

Close-up view of interferograms (14 August 2019 - 10 April 2020) estimated by MLE-PL and S-MLE-PL in case $l = 20$ and $n = 64$

Content

Conclusion

Conclusion

- **Novel approach:** efficient incorporation of new SAR images within a PL framework
- **Performance:** matches that of offline approaches
- **Cost:** Lower computational costs than traditional offline approaches

Perspectives

- Generalization of $\mathrm{S\text{-}MLE\text{-}PL}$ to a bloc of new SAR images
- Proceed to step 2 : estimate the displacement time series and compare the results with GPS data

Ongoing works

- Robust $\mathrm{S\text{-}MLE\text{-}PL}$: Generalization to a non gaussian model [4]
- Approach 2 : Sequential phase estimation based on a covariance fitting problem [5] $\longrightarrow$ MM algorithm, Remannian gradient descent ...

[1] T. W. Anderson. *An introduction to multivariate statistical analysis*, volume 2. Wiley New York, 1958.

[2] A. Guarnieri and S. Tebaldini. On the exploitation of target statistics for sar interferometry applications. *IEEE Transactions on Geoscience and Remote Sensing*, 46(11):3436–3443, 2008.

[3] D. E. hajjar, Y. Yan, G. Ginolhac, and M. E. korso. Sequential phase linking: progressive integration of sar images for operational phase estimation. In *IGARSS 2024 IEEE International Geoscience and Remote Sensing Symposium*. IEEE, 2024 (accepted).

[4] P. Vu, A. Breloy, F. Brigui, Y. Yan, and G. Ginolhac. Robust phase linking in insar. *IEEE Transactions on Geoscience and Remote Sensing*, 2023.

[5] P. Vu, A. Breloy, F. Brigui, Y. Yan, and G. Ginolhac. Covariance fitting interferometric phase linking: Modular framework and optimization algorithms. *arXiv preprint arXiv:2403.08646*, 2024.

[6] P. Vu, F. Brigui, A. Breloy, Y. Yan, and G. Ginolhac. A new phase linking algorithm for multi-temporal insar based on the maximum likelihood estimator. In *IGARSS International Geoscience and Remote Sensing Symposium*, pages 76–79. IEEE, 2022.

Thank you for your attention !

This work is funded by the ANR REPED-SARIX project (ANR-21-CE23-0012-01) of the French national Agency of research.

Appendix - S-MLE-PL simulations

Simulation parameters

- $\widetilde{\boldsymbol{\Psi}}$: Toeplitz matrix with coherence coefficient $\rho \in [0.5, 0.7, 0.9]$
- $l = 20$ SAR phases: random values in $[-\pi, \pi]$
- Covariance matrix : $\widetilde{\boldsymbol{\Sigma}} = \text{diag}(\widetilde{\mathbf{w}}_\theta)\widetilde{\boldsymbol{\Psi}}\text{diag}(\widetilde{\mathbf{w}}_\theta)^H$
- n i.i.d samples simulated following the $\mathcal{CN}(0, \widetilde{\boldsymbol{\Sigma}})$

Approaches to be compared

- 2p-InSAR : phase estimated from n-pixel averaged interferograms formed with respect to the first image
- classic PL
- MLE-PL
- S-MLE-PL (our approach)

Appendix - S-MLE-PL simulations results

Gaussian distributed input data

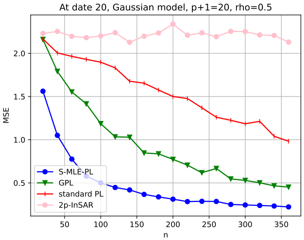

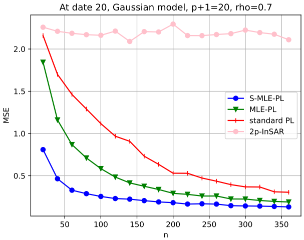

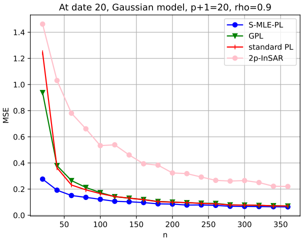

MSE of InSAR phases estimates using 2p-InSAR, classic PL and $\mathrm{MLE\text{-}PL}$ and $\mathrm{S\text{-}MLE\text{-}PL}$ with Gaussian distributed input data where $l = 20$, $\rho \in [0.5, 0.7, 0.9]$, using 1000 Monte Carlo trials

Appendix - Sequential integration of several new images

Approaches to be compared

- $\mathrm{MLE\text{-}PL}$ processing all t images
- $\mathrm{S\text{-}MLE\text{-}PL}$ where the $l = p + 1$ past phases are computed using $\mathrm{MLE\text{-}PL}$
- $\mathrm{S\text{-}MLE\text{-}PL}$ where the $l = p + 1$ past phases consist of p phases calculated using $\mathrm{MLE\text{-}PL}$ approach and $(p + 1)^{\text{th}}$ phase calculated using $\mathrm{S\text{-}MLE\text{-}PL}$

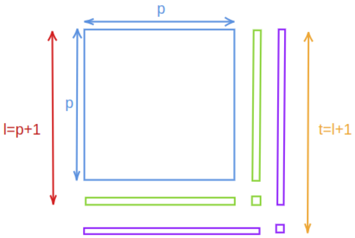

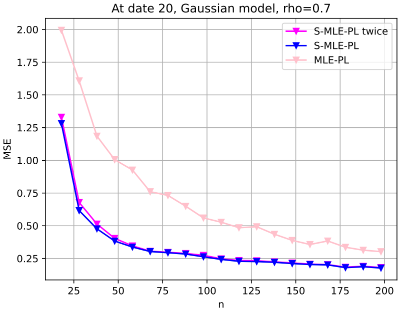

Appendix - Quality assessment of phase estimation

$$\gamma_{\text{post}} = \frac{\mathrm{Re}\left(\sum_{q=1}^{l}\sum_{i=q+1}^{l} \mathrm{e}^{(\delta\theta_{iq}-(\hat{\theta}_i-\hat{\theta}_q))}\right)}{l(l-1)/2}$$

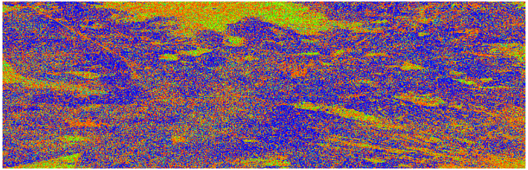

MLE-PL

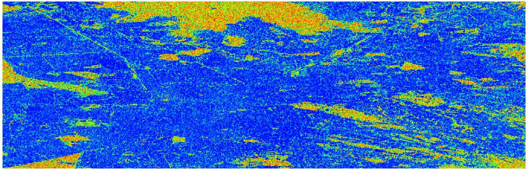

S-MLE-PL

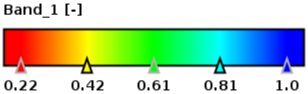

Appendix - COFI-PL

Covariance fitting interferometric PL (COFI-PL) involves refining the structure of the covariance matrix estimator by minimizing a projection criterion.

The fitting problem can be reformulated as [5]

$$\begin{aligned} \underset{\widetilde{\mathbf{w}}_\theta}{\text{minimize}} \quad & f(\widetilde{\boldsymbol{\Sigma}}, \widetilde{\boldsymbol{\Psi}} \odot \widetilde{\mathbf{w}}_\theta \widetilde{\mathbf{w}}_\theta^H) \\ \text{subject to} \quad & \theta_1 = 0 \\ & \widetilde{\mathbf{w}}_\theta \in \mathbb{T}_p \end{aligned} \tag{5}$$

with $\mathbb{T}_p = \{\mathbf{w} \in \mathbb{C}^p | |[w]_i| = 1, \forall i \in [1, p]\}$

Solution

- MM algorithm
- Riemannian gradient descent algorithm

[5] Vu, Phan Viet Hoa, et al. "Covariance Fitting Interferometric Phase Linking: Modular Framework and Optimization Algorithms." arXiv preprint arXiv:2403.08646 (2024).

Appendix - Matrix distances and Covariance estimation

Matrix distances

- Kullback-Leibler divergence : $f^{KL}_{\widetilde{\boldsymbol{\Sigma}}}(\widetilde{\mathbf{w}}_\theta) = \widetilde{\mathbf{w}}_\theta^H(\widetilde{\boldsymbol{\Psi}}^{-1} \odot \widetilde{\boldsymbol{\Sigma}})\mathbf{w}_\theta$
- Frobenius norm : $f^{LS}_{\widetilde{\boldsymbol{\Sigma}}}(\widetilde{\mathbf{w}}_\theta) = -2\widetilde{\mathbf{w}}_\theta^H(\widetilde{\boldsymbol{\Psi}} \odot \widetilde{\boldsymbol{\Sigma}})\widetilde{\mathbf{w}}_\theta$
- ...

Covariance estimation

- SCM : $\widetilde{\boldsymbol{\Sigma}} = \frac{1}{n}\sum_{i=1}^{n} \widetilde{\mathbf{x}}^i \widetilde{\mathbf{x}}^{iH}$
- Phase-Only : $\widetilde{\boldsymbol{\Sigma}} = \frac{1}{n}\sum_{i=1}^{n} \widetilde{\mathbf{y}}^i \widetilde{\mathbf{y}}^{iH}$ with $\widetilde{\mathbf{y}} = \phi(\widetilde{\mathbf{x}})$ with $\Phi : \widetilde{x} = \gamma e^{i\theta} \rightarrow e^{i\theta}$
- Shrinkage to identity : $\widetilde{\boldsymbol{\Sigma}}(\beta) = \beta\hat{\boldsymbol{\Sigma}} + (1-\beta)\frac{\mathrm{tr}(\hat{\boldsymbol{\Sigma}})}{p}\mathbf{I}$ with $\beta \in [0,1]$
- Covariance matrix tapering : $\widetilde{\boldsymbol{\Sigma}}(\beta) = \mathbf{W}(b) \odot \hat{\boldsymbol{\Sigma}}$ with $[\mathbf{W}(b)]_{ij} = \begin{cases} 1 & \text{if} \quad |i-j| \leq b \\ 0 & \text{otherwise} \end{cases}$

Data model

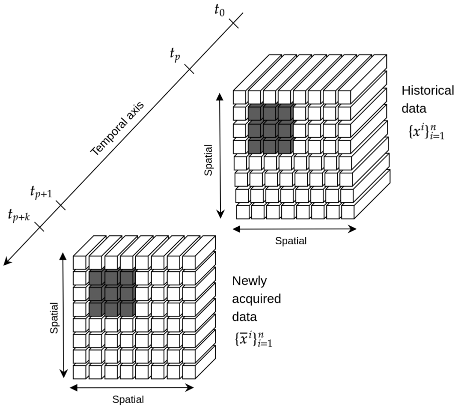

Representation of time series of SAR data with a sliding window containing n pixels $\tilde{\mathbf{x}}^i$.

We consider a set $\{\tilde{\mathbf{x}}^i\}_{i=1}^n$ where

$$\tilde{\mathbf{x}}^i = [\underbrace{x_1^i, \ldots, x_p^i}_{\mathbf{x}^i}, \underbrace{x_{p+1}^i, \ldots, x_{p+k}^i}_{\bar{\mathbf{x}}^i}]^T \in \mathbb{C}^{p+k} \quad (6)$$

Each pixel of the local patch is assumed to be distributed as a zero mean CCG, i.e., $\tilde{\mathbf{x}} \sim \mathcal{CN}(0, \widetilde{\mathbf{\Sigma}})$. The hermitian structured covariance matrix, can be rewritten as

$$\widetilde{\mathbf{\Sigma}} = \begin{pmatrix} \Sigma_{\text{past}} & \mathbf{V}^H \\ \mathbf{V} & \mathbf{Z} \end{pmatrix}_{(p+k,p+k)}$$

The coherence matrix $\widetilde{\mathbf{\Psi}}$ can be represented as follow :

$$\widetilde{\mathbf{\Psi}} = \begin{pmatrix} \Psi_{\text{past}} & \mathbf{A}^T \\ \mathbf{A} & \mathbf{B} \end{pmatrix}_{(p+k,p+k)}$$